Scaling Relations in Coronal Mass Ejections and Energetic Proton Events associated with Solar Superflares

Takuya Takahashi[1], Yoshiyuki Mizuno[2], Kazunari Shibata[1]

takahasi@kusastro.kyoto-u.ac.jp

ABSTRACT

In order to discuss the potential impact of solar 'superflares' on space weather, we investigated statistical relations among energetic proton peak flux with energy higher than 10MeV (F_p), CME speed near the Sun (V_{CME}) obtained by *SOHO*/LASCO coronagraph and flare soft X-ray peak flux in 1-8Åband (F_{SXR}) during 110 major solar proton events (SPEs) recorded from 1996 to 2014. The linear regression fit results in the scaling relations $V_{CME} \propto F_{SXR}^{\alpha}$, $F_p \propto F_{SXR}^{\beta}$ and $F_p \propto V_{CME}^{\gamma}$ with $\alpha = 0.30 \pm 0.04$, $\beta = 1.19 \pm 0.08$ and $\gamma = 4.35 \pm 0.50$, respectively. On the basis of simple physical assumptions, on the other hand, we derive scaling relations expressing CME mass (M_{CME}), CME speed and energetic proton flux in terms of total flare energy (E_{flare}) as, $M_{CME} \propto E_{flare}^{2/3}$, $V_{CME} \propto E_{flare}^{1/6}$ and $F_p \propto E_{flare}^{5/6} \propto V_{CME}^{5}$, respectively. We then combine the derived scaling relations with observation, and estimated the upper limit of V_{CME} and F_p to be associated with possible solar superflares.

Subject headings: Sun: coronal mass ejections —Sun: flares — solar-terrestrial relations — Stars: activity

1. Introduction

Solar flares are the biggest explosion in the solar system where magnetic field energy stored in the active region corona is rapidly released through magnetic reconnection process (Shibata & Magara 2011; Hudson 2011). During flares, coronal plasma is sometimes ejected out into the interplanetary space (coronal mass ejections; CMEs) (Illing & Hundhausen 1986;

[1] Kwasan and Hida Observatories, Kyoto University, Yamashina, Kyoto 607-8471, Japan.

[2] Faculty for the Study of Contemporary Society, Kyoto Women's University, 35 Kitahiyoshi-cho, Imakumano, Higashiyama-ku, Kyoto 605-8501 Japan

Gopalswamy 2009). Significant portion of active region magnetic field energy released during flares is converted to the kinetic energy of CMEs (Emslie et al. 2012). The resultant plasma and magnetic field structures detected at 1 AU are called interplanetary CMEs (ICMEs)(Zhang et al. 2007). When helical magnetic field of ICME ejecta (magnetic cloud) or draped magnetic field in the interplanetary sheath ahead of magnetic cloud have strong southward component, geomagnetic storms occur (Klein & Burlaga 1982; Tsurutani et al. 1988).

Energetic protons are accelerated both at CME-driven shocks and flare site (Reames et al. 1996; Tsurutani et al. 2009). In the case of shock acceleration mechanism, the efficiency of particle acceleration depends on shock Mach number and its normal direction, and particles are known to be most efficiently accelerated when the shocks are quasi-parallel (Kennel et al. 1984a; Tsurutani & Lin 1985). Accelerated particles arrive at Earth when Earth is magnetically well connected to the shock front (solar proton event; SPE). Shock acceleration mechanism is generally thought to be dominant of the two, but extremely high energy protons (with energy $\sim$ GeV) accelerated at the flare site right after the flare onset are discussed to be responsible for the prompt component of Ground Level Enhancement (GLE) events (Aschwanden 2012).

Large SPEs are often associated with large solar flares or fast CMEs (Gopalswamy et al. 2004). The largest SPE after 1970 in terms of $E > 10$ MeV proton peak flux occurred on 4 August 1972. The estimated $E > 10$ MeV proton peak flux is higher than 6×10^4 pfu (particle flux unit; particles sr^{-1} cm^{-2} s^{-1}) (Kurt et al. 2004). Modern extreme events that occurred on 23 July 2012 recorded the peak $E > 10$ MeV proton flux of 6.5×10^4 pfu observed with STEREO-A space craft when interplanetary shock wave passed the space craft (Gopalswamy et al. 2014).

CMEs and SPEs are the two main drivers of hazardous space weather outcomes such as potential radiation hazards for space astronauts, geomagnetic storms and telecommunication failures (Loomis 1861; Tsurutani et al. 2003). On the other hand, fast CMEs and intense energetic protons might have had important influence on ancient terrestrial environment through chemical processes in the terrestrial atmosphere (Airapetian et al. 2016). Young stars (like our ancient Sun) which rotate very rapidly are known to frequently produce superflares (10-10^4 times more energetic flares than the largest solar flares ever observed) possibly due to its active dynamo. Recent observation by Kepler satellite revealed that some solar-type stars with rotation period longer than 10 days can also produce superflares though not very frequent (Maehara et al. 2012).

The most widely used index of solar flare magnitude is soft X-ray (SXR) peak flux monitored by GOES satellite in 1-8Å passband. The proportionality between hard X-ray

(HXR) fluence and SXR peak flux of indivisual flares is known as Neupert effect, and it is thought to be a casual index of released magnetic field energy during flares (Neupert 1968). The solar flares are known to follow the frequency distribution of power-law form in terms of SXR peak flux (Yashiro et al. 2006). The largest ever solar flare observed in X-ray that occurred on 4 November 2003 saturated the *GOES* X-ray detector in 1-8Å passband. The estimated flare class by linear extrapolation is X28, while X-ray class estimation based on ionosphereic response resulted in X45 $\pm$ 5 (Thomson et al. 2004). Evidence of a spike of carbon-14 isotope between 774-775 is discovered from tree rings indicative of huge solar energetic particle event driven by solar superflares (Miyake et al. 2012). Gopalswamy et al. (2010) estimated maximum flare energy to be of order 10^{35} erg (flare of $\sim$X1,000 class) based on observed maximum magnetic field strength in a sunspot and largest AR size. They estimated maximum CME speed associated with such a largest class of flares to be 7,200 km s^{-1} assuming the CME mass to be of order 10^{18} g (Gopalswamy 2011).

There are studies on statistical relations among flare SXR peak flux observed with *GOES* (F_{SXR}), CME speed near the Sun (V_{CME}) and $E > 10$ MeV proton peak number flux (F_p) from various datasets. F_p is known to be correlated both with V_{CME} and F_{SXR} (Gopalswamy 2011; Gopalswamy et al. 2003). From 19 SPEs occurred during maximum to minimum of solar cycle 23, Gopalswamy et al. (2003) reported statistical relation, $F_p \propto V_{CME}^{3.7}$ and $F_p \propto F_{SXR}^{0.63}$, respectively. Also, the correlation coefficients of F_{SXR} and V_{CME} for events during 1996-2007 and GLE events are reported to be 0.37 and 0.50, respectively (Yashiro & Gopalswamy 2009; Gopalswamy et al. 2012). The correlation between F_{SXR} and kinetic energy of CME ($K = M_{CME}V_{CME}^2/2$ with M_{CME} being CME mass estimated from coronagraph observations) are also reported (Gopalswamy 2009).

In this paper, we analyzed the statistical relations among CME speed, peak energetic proton flux and flare SXR peak flux from a single list of events, i.e. 110 SPEs recorded from 1996 to 2014 whose peak proton flux in the E > 10MeV channel of GOES satellite exceeded 10 pfu. We derive scaling relations among CME speed, energetic proton flux and flare SXR peak flux on the basis of simple assumptions and compared with observation.

Finally, we estimate how fast CMEs will be, and how intense proton flux will come during possible solar superflare events based on the combination of the scaling relations and observation.

2. Dataset

A total of 143 major SPEs were recorded from 1996 to 2014 whose peak proton flux in the E > 10MeV channel of *GOES* satellite exceeded 10 pfu. The events are listed in CDAW major SEP event list page.[1] For 110 out of 143 SPEs, both flare SXR peak flux and CME speeds near the Sun accompanied with the SPEs are determined with X-ray Sensor on board the *GOES* satellite and Large Angle and Spectrometric Coronagraph (LASCO; Brueckner et al. 1995) on board the Solar and Heliospheric Observatory (*SOHO*; Domingo et al. 1995), respectively. For 80 out of these 110 SPEs, the mass of accompanied CMEs are also determined with LASCO. The estimated speed and mass of CMEs are obtained from CDAW Data Center CME catalog (Yashiro et al. 2004), which is also available online.[2]

3. Statistical relations among flare SXR peak flux, CME speed and energetic proton flux

We study statistical relation among F_{SXR} and F_p during 110 major SPEs recorded between 1996 and 2014. Most CMEs, namely 92 out of 110, were 'halo' ones. A 'halo' CME is an expanding plasma of CME that appears to form a halo of enhanced brightness completely surrounding the occulting disk when observed with a coronagraph (Howard et al. 1982). The estimation of speed and mass of halo CMEs by coronagraph observations generally contains large uncertainty. We neglect the uncertainty of speed and mass estimation based on coronagraph observations throughout the analysis.

In Figure 1, we show correlation plot of F_p and F_{SXR}. A regression line is drawn as a solid line to fit the log-log data plot. We used ordinary least squares (OLS) bisector method for linear regressions hereafter, which is suitable for the discussion of underlying functional relation between two quantities (Isobe et al. 1990). The correlation coefficient was $r = 0.41$, and the linear regression fit gives $F_p \propto F_{SXR}^{\beta}$ with $\beta = 1.19 \pm 0.08$. 5 out of 110 SPEs had F_p larger than 10^4 pfu, and 4 out of the five were associated with X class flares.

F_p also correlates with V_{CME} in our data set(Figure 2). We note here that throughout the paper, the CME speed V_{CME} refers to the estimated speed of CME near the Sun based on observation with *SOHO*/LASCO. The average CME speed of all the 110 events was 1566 km s^{-1}, and the average CME speed of 5 most intense SPEs was 2016 km s^{-1}. The correlation coefficient between F_p and V_{CME} for our dataset was $r = 0.45$, and the linear

[1]http://cdaw.gsfc.nasa.gov/CME_list/sepe/

[2]http://cdaw.gsfc.nasa.gov/CME_list/

regression result gives $F_p \propto V_{CME}^{\gamma}$ with $\gamma = 4.35 \pm 0.50$. The event with $F_p = 1860$ pfu and V_{CME} =882 km s^{-1} shown as unfilled circle in Figure 2 seems to be an outlier, and the analysis without the event makes the correlation coefficient a little bit higher and the slope a little steeper, namely, $r = 0.48$ and $\gamma = 4.50 \pm 0.48$, respectively. The event shown as unfilled circle was associated with an X7.1 class solar flare, and the CME was a Halo one.

Figure 3 shows correlation plot between V_{CME} and F_{SXR}. The correlation coefficient was 0.42, and the linear regression result gives $V_{CME} \propto F_{SXR}^{\alpha}$ with $\alpha = 0.30 \pm 0.04$. In 80 SPEs out of 110 analyzed here, CME mass M_{CME} is also estimated[3]. Correlation between M_{CME} and F_{SXR} in the 80 SPEs was very poor with $r = -0.02$, possibly due to large uncertainty in mass estimation of halo CMEs.

4. Scaling relations between flare magnitude, CME speed, CME mass and peak proton flux

We try to express CME mass (M_{CME}), CME speed (V_{CME}) and energetic proton peak flux (F_p) as a power-law form of total released energy during flares (E_{flare}) based on three simple physical assumptions. First, we assume the CME mass is the sum of the mass within gravitationally stratified active region (AR) corona,

$$M_{CME} = L^2 \int_0^L \rho_0 \exp(-\frac{z}{H}) dz \sim \rho_0 L^2 H \quad (1)$$

where ρ_0, L and H are the density at the base of the AR corona, the length scale of flaring AR and the pressure scale hight, respectively. We implicitly assumed AR corona size L is much larger than the coronal scale height H, which is suitable for large AR where large flares can occur.

Next, we assume CME kinetic energy is proportional to the total energy released during the flare, which is also a constant fraction f of AR magnetic field energy (Emslie et al. 2012),

$$E_{CME} = \frac{1}{2} M_{CME} V_{CME}^2 \propto E_{flare} = f \frac{1}{8\pi} B_0^2 L^3 \quad (2)$$

where E_{flare} and E_{CME} are the total released energy during flares and CME kinetic energy respectively. B_0 is the active region magnetic field strength. Typical magnetic field strength of sunspots is of the order of 3000 G.

[3]http://cdaw.gsfc.nasa.gov/CME_list/

The first and second assumptions (equations (1) and (2)) lead to the following relations.

$$M_{CME} \propto E_{flare}^{2/3}, \tag{3}$$

$$V_{CME} \propto E_{flare}^{1/6}. \tag{4}$$

Aarnio et al. (2011) studied CME/flare pairs observed with LASCO and *GOES* occurred from 1996 to 2006 and found the statistical relationship $M_{CME} \propto F_{SXR}^{0.7}$. Aarnio et al. (2012) further discussed the statistical relation of CME mass M_{CME} and energy released in the form of SXR during flares E_{SXR} of the form $M_{CME} = K_M E_{SXR}^{\delta}$, where $K_M = (2.7 \pm 1.2) \times 10^{-3}$ in cgs units, and $\delta = 0.63 \pm 0.04$. Such observations seem to be consistent with our scaling relation of $M_{CME} \propto E_{flare}^{2/3}$. Very interestingly, such scaling relation between M_{CME} and F_{SXR} obtained from solar flare statistics is consistent with mega-flare observation on young T Tauri star implying the scaling relation holds in a very wide energy range, that is more than 10 orders of magnitude in flare energy (Aarnio et al. 2012).

We then try to relate energetic proton peak flux F_p with flare energy E_{flare}. We assume that the total kinetic energy of solar energetic protons E_p is proportional to flare energy, and the duration of proton flux enhancement is determined by CME propagation timescale $t_{CME} \propto L/V_{CME}$.

$$E_p \propto F_p t_{CME} \propto E_{flare} \tag{5}$$

From equation (4) and (5) we express F_p as follows.

$$F_p \propto E_{flare}^{5/6} \propto V_{CME}^5 \tag{6}$$

In the derivation, we neglect the proton energy spectral variation depending on flare magnitude.

The scaling relation (6) $F_p \propto V_{CME}^5$ is plotted as a dashed line in Figure 2 and compared with the observed correlation. The linear regression fit in double logarithmic space was $F_p \propto V_{CME}^{\gamma}$ with $\gamma = 4.35 \pm 0.50$ which has a slightly smaller slope compared to (6).

5. Estimation of CME speed and proton flux associated with solar superflares

In this section, we compare the scaling relations derived above with observational statistical relations, and try to estimate how fast CME and how intense proton flux will result in the case of solar superflares.

Emslie et al. (2012) discussed that kinetic energy of CME is comparable with flare energy, namely $E_{CME} \sim E_{flare}$.

Figure 4 shows the correlation between CME kinetic energy estimated from LASCO observation by $E_{CME} = 1/2 M_{CME} V_{CME}^2$ and flare SXR peak flux F_{SXR} associated with 80 major SPEs with CME mass estimation.The correlation coefficient was $r = 0.28$ and the linear regression with OLS bisector method results in $E_{CME} \propto F_{SXR}^{\epsilon}$ with $\epsilon = 0.80 \pm 0.07$.

In order to estimate the upper-limit of CME speed and energetic proton flux in response to SXR class of solar flares, we try to relate V_{CME} and F_p with F_{SXR} by assuming F_{SXR} is roughly proportional to total released energy during flares, namely $F_{SXR} \propto E_{flare}$.

Based on this assumption, F_p and V_{CME} are respectively scaled with F_{SXR} as

$$V_{CME} \propto F_{SXR}^{1/6}, \tag{7}$$

$$F_p \propto F_{SXR}^{5/6}. \tag{8}$$

Scaling relations (7) and (8) are shown as dashed lines in Figures 3 and 1, respectively. The dashed lines are positioned in each plots so that they pass through the upper-left-most SPE, in order that we can discuss the upper limit of CME speed ($V_{CME,upperlimit}$) and proton flux ($F_{p,upperlimit}$) in response to F_{SXR}. Explicit formulas are as follows,

$$V_{CME,upperlimit} = V_0 F_{SXR}^{1/6}, \tag{9}$$

$$F_{p,upperlimit} = F_{p,0} F_{SXR}^{5/6}, \tag{10}$$

where $V_0 = 1.3 \times 10^4$ km s^{-1}, $F_{p,0} = 10^{7.83}$ pfu and F_{SXR} is normalized in unit of 1 W m^{-2}.

Compared with linear regression fits, namely, $V_{CME} \propto F_{SXR}^{\alpha}$ and $F_p \propto F_{SXR}^{\beta}$ with $\alpha = 0.30 \pm 0.04$, $\beta = 1.19 \pm 0.08$, the derived scaling relations had gentler slopes of $1/6 \simeq 0.17$ and $5/6 \simeq 0.83$, respectively. We note that in Figures 3 and 1, the scaling relations (7) and (8) seem consistent with the line of the upper limit of observed V_{CME} and F_p with respect to F_{SXR}.

From equation (9), the upper limit of V_{CME} for X10, X100 and X1000 solar flares will be $V_{CME,X10} = 4.2 \times 10^3$ km s^{-1}, $V_{CME,X100} = 6.2 \times 10^3$ km s^{-1} and $V_{CME,X1000} = 9.1 \times 10^3$ km s^{-1}, respectively (Figure 5 (a)). From equation (10), the upper limit of F_p for X10, X100 and X1000 solar flares will be $F_{p,X10} = 2.0 \times 10^5$ pfu, $F_{p,X100} = 1.6 \times 10^6$ pfu and $F_{p,X1000} = 1.0 \times 10^7$ pfu, respectively (Figure 5 (b)).

6. Impact of superflare-associated CMEs and SPEs on space weather and terrestrial environment

In this paper we studied CME properties and energetic proton flux associated with possible superflares on the Sun. The scaling relations expressing M_{CME}, V_{CME} and F_p in terms of E_{flare} derived from simple assumptions are not inconsistent with statistical relations from solar observation. On the basis of the analysis above, we expect CMEs associated with superflares to be fast and heavy, which will have a huge impact on space weather (Loomis 1861; Tsurutani et al. 2003).

Huge geomagnetic storms are initiated by magnetic reconnection between injected southward magnetic field of ICMEs $B_{s,ICME}$ and Earth's northward magnetic field (Dungey 1961; Gonzalez et al. 1994). When ICME magnetic field is northward, no geomagnetic storms occur (Tsurutani & Gonzalez 1995). The magnitude of geomagnetic storms is mainly determined by solar wind westward electric field $E_y \sim V_{ICME,1AU} B_{s,ICME}$, where $V_{ICME,1AU}$ is ICME speed near Earth(Burton et al. 1975; Gonzalez et al. 1994). The upperlimit of the magnetic field strength of magnetic cloud $B_{s,MC}$ is estimated by the balance of magnetic pressure and dynamic pressure as $B_{s,MC}^2/8\pi \sim 1/2\rho_{SW}(V_{ICME,1AU} - V_{SW})^2 \sim 1/2\rho_{SW}V_{ICME,1AU}^2$, where ρ_{SW} and V_{SW} are density and speed of the solar wind near Earth. If we assume typical value range of solar wind proton number density at 1 AU, namely, $n_p = 3 - 8$ cm^{-3} (Schwenn 1990), $B_{s,MC}$ is estimated as $B_{s,MC} \sim (0.08 - 0.13)$ $(V_{ICME,1AU}/1\ kms^{-1})$ nT. This is consistent with observationally known fact that magnetic clouds with higher peak speed (v_{peak}) also possess stronger core magnetic field (B_{peak}), with observational statistical relation $B_{peak} = 0.047(v_{peak}/1\ kms^{-1})$ nT (Gonzalez et al. 1998). The upper limit of westward electric field E_y is estimated as $E_y \sim \sqrt{4\pi\rho_{SW}}V_{CME,1AU}^2$.

CMEs are decelerated during their propagation in the interplanetary space (Gopalswamy et al. 2001), sweeping up the interplanetary plasma on their path. We expect from conservation of momentum that if a CME ejecta is heavy enough (comparable to or heavier than the mass scraped up on its path), the CME will not be decelerated much. Fast and heavy ICMEs with southward magnetic field associated with solar superflares would cause extreme geomagnetic storms.

Extreme increase of radiation levels in space associated with solar superflares also result in the increase of radiation at the flight altitude and sometimes at the sea level (Ground Level Enhancement; GLE) through airshower formation in Earth's atmosphere. The radiation levels in Earth atmosphere depend on high energy component of energetic proton flux in space. For example, GLEs are mainly caused by energetic protons injected to the top of the atmospheric layer whose energy is higher than ~ 1 GeV. The maximum energy of energetic protons associated with solar flares are known to be less than several GeV.

We estimate the maximum possible energy of energetic protons accelerated at CME-driven shocks. If we apply Hillas limit (Hillas 1984), we get the estimation of proton maximum energy as $E_{max} \sim 2$ GeV $B_{0.1}V_{3000}L_{1Rs}$, where $B_{0.1}$, V_{3000} and L_{1Rs} are the upstream magnetic field strength in unit of 0.1 G, shock propagation speed in unit of 3000 km s^{-1}

and length scale of acceleration site in unit of the solar radius, respectively. If we assume L is independent of flare energy, we obtain, $E_{max} \propto V_{CME} \propto E_{flare}^{1/6}$. On the other hand, if we assume protons with highest energies are accelerated by the electric voltage generated by magnetic reconnection at flare site, we obtain $E_{max} \sim 7$ GeV $B_{100}V_{100}L_{0.1Rs}$, where B_{100}, V_{100} and $L_{0.1Rs}$ are the active region magnetic field strength in unit of 100 G, plasma 'inflow' speed in unit of 100 km s^{-1} and length scale of the flaring active region in unit of 0.1 solar radius, respectively. Generally, magnetic reconnection rate $\sim V_{in}/V_{CME}$ is independent of flare magnitude (Shibata & Magara 2011). Applying equation (2) and (4), we obtain $E_{max} \propto E_{flare}^{1/2}$. X1000 class flare, for example, may produce 10 GeV protons which result in drastic increase of radiation level in Earth atmospheric layer.

In the derivation of scaling relation (6), we assumed the relation $t_{CME} \propto L/V_{CME}$, where L is the active region size. If we use constant length scale L_0 in place of L, the scaling relation would change to $F_p \propto E_{flare}^{7/6} \propto V_{CME}^{7}$. This might be the case if the particles are accelerated at the shock front in the interplanetary space where physical quantities do not depend on active region size.

The CME catalog we used in this study is generated and maintained at the CDAW Data Center by NASA and The Catholic University of America in cooperation with the Naval Research Laboratory. SOHO is a project of international cooperation between ESA and NASA. We studied SPEs from online SPE catalog provided by the CDAW Data Center[4]. This work was supported by JSPS KAKENHI Grant Numbers 16H03955. The authors are grateful to Dr. Seiji Yashiro for providing valuable information and giving us fruitful comments on data handling. This work is motivated partly by Mr. Taira Hiraishi's master thesis.

REFERENCES

Aarnio, A. N., Matt, S. P., & Stassun, K. G. 2012, ApJ, 760, 9

Aarnio, A. N., Stassun, K. G., Hughes, W. J., & McGregor, S. L. 2011, Sol. Phys., 268, 195

Airapetian, V. S., Glocer, A., Gronoff, G. et al. 2016, Nature Geoscience, 9, 452

Aschwanden, M. J. 2012, Space Sci. Rev., 171, 3

[4]http://cdaw.gsfc.nasa.gov/CME_list/sepe/

Burton, R., R. McPherron, and C. Russell 1975, Journal of Geophysical Research (Space Physics), 80, 4204-4214

Dungey, J. W. 1961, Physical Review Letters, 6, 47

Emslie, A. G., Dennis, B. R., Shih, A. Y., et al. 2012, ApJ, 759, 71

Gonzalez, W. D., Joselyn, J. A., Kamide, Y., et al. 1994, J. Geophys. Res., 99, 5771

Gonzalez, W. D., de Gonzalez, A. L. C., Dal Lago, A., et al. 1998, Geophys. Res. Lett., 25, 963

Gopalswamy, N., Lara, A., Yashiro, S., Kaiser, M. L., & Howard, R. A. 2001, J. Geophys. Res., 106, 29207

Gopalswamy, N., Yashiro, S., Kaiser, M. L., & Howard, R. A. 2003, Advances in Space Research, 32, 2613

Gopalswamy, N., Yashiro, S., Lara, A., et al. 2003, Geophys. Res. Lett., 30, 8015

Gopalswamy, N., Yashiro, S., Krucker, S., Stenborg, G., & Howard, R. A. 2004, Journal of Geophysical Research (Space Physics), 109, A12105

Gopalswamy, N. 2009, Climate and Weather of the Sun-Earth System (CAWSES)

Gopalswamy, N., Akiyama, S., Yashiro, S., & Mäkelä, P. 2010, Astrophysics and Space Science Proceedings, 19, 289

Gopalswamy, N. 2011, Astronomical Society of India Conference Series, 2,

Gopalswamy, N., Xie, H., Yashiro, S., et al. 2012, Space Sci. Rev., 171, 23

Gopalswamy, N., Xie, H., Akiyama, S., Mäkelä, P. A., & Yashiro, S. 2014, Earth, Planets, and Space, 66, 104

Gopalswamy, N., Yashiro, S., Xie, H., Akiyama, S., & Mäkelä, P. 2015, Journal of Geophysical Research (Space Physics), 120, 9221

Hillas, A. M. 1984, ARA&A, 22, 425

Howard, R. A., Michels, D. J., Sheeley, N. R., Jr., & Koomen, M. J. 1982, ApJ, 263, L101

Hudson, H. S. 2011, Space Sci. Rev., 158, 5

Illing, R. M. E., & Hundhausen, A. J. 1986, J. Geophys. Res., 91, 10951

Isobe, T., Feigelson, E. D., Akritas, M. G., & Babu, G. J. 1990, ApJ, 364, 104

Kennel, C. F., Edmiston, J. P., Russell, C. T., et al. 1984, J. Geophys. Res., 89, 5436

Klein, L. W., & Burlaga, L. F. 1982, J. Geophys. Res., 87, 613

Kurt, V., Belov, A., Mavromichalaki, H., & Gerontidou, M. 2004, Annales Geophysicae, 22, 2255

Livingston, W., Harvey, J. W., Malanushenko, O. V., & Webster, L. 2006, Sol. Phys., 239, 41

Loomis, Elias, 1861, American Journal of Science 96, 318

Maehara, H., Shibayama, T., Notsu, S., et al. 2012, Nature, 485, 478

Miyake, F., Nagaya, K., Masuda, K., & Nakamura, T. 2012, Nature, 486, 240

Neupert, W. M. 1968, ApJ, 153, L59

Reagan, Joseph B., William L. Imhof, & Vincent F. Moughan. 1973, LOCKHEED MISSILES AND SPACE CO INC PALO ALTO CA PALO ALTO RESEARCH LAB, No. LMSC-D352207

Reames, D. V., Barbier, L. M., & Ng, C. K. 1996, ApJ, 466, 473

Reames, D. V. 2000, 26th International Cosmic Ray Conference, ICRC XXVI, 516, 289

Schrijver, C. J., Beer, J., Baltensperger, U., et al. 2012, Journal of Geophysical Research (Space Physics), 117, A08103

Schwenn, R. 1990, Physics of the Inner Heliosphere I, 99

Shibata, K., & Magara, T. 2011, Living Reviews in Solar Physics, 8, 6

Thomson, N. R., Rodger, C. J., & Dowden, R. L. 2004, Geophys. Res. Lett., 31, L06803

Tsurutani, B. T., Smith, E. J., Gonzalez, W. D., Tang, F., & Akasofu, S. I. 1988, J. Geophys. Res., 93, 8519

Tsurutani, B. T., & Gonzalez, W. D. 1990, J. Geophys. Res., 95, 12305

Tsurutani, B. T., & Gonzalez, W. D. 1995, Geophys. Res. Lett., 22, 663

Tsurutani, B. T., & Lin, R. P. 1985, J. Geophys. Res., 90, 1

Tsurutani, B. T., Gonzalez, W. D., Lakhina, G. S., & Alex, S. 2003, Journal of Geophysical Research (Space Physics), 108, 1268

Tsurutani, B. T., Verkhoglyadova, O. P., Mannucci, A. J., et al. 2009, Radio Science, 44, RS0A17

Yashiro, S., Gopalswamy, N., Michalek, G., et al. 2004, Journal of Geophysical Research (Space Physics), 109, A07105

Yashiro, S., Akiyama, S., Gopalswamy, N., & Howard, R. A. 2006, ApJ, 650, L143

Yashiro, S., & Gopalswamy, N. 2009, Universal Heliophysical Processes, 257, 233

Zhang, J., Richardson, I. G., Webb, D. F., et al. 2007, Journal of Geophysical Research (Space Physics), 112, A10102

This preprint was prepared with the AAS LaTeX macros v5.2.

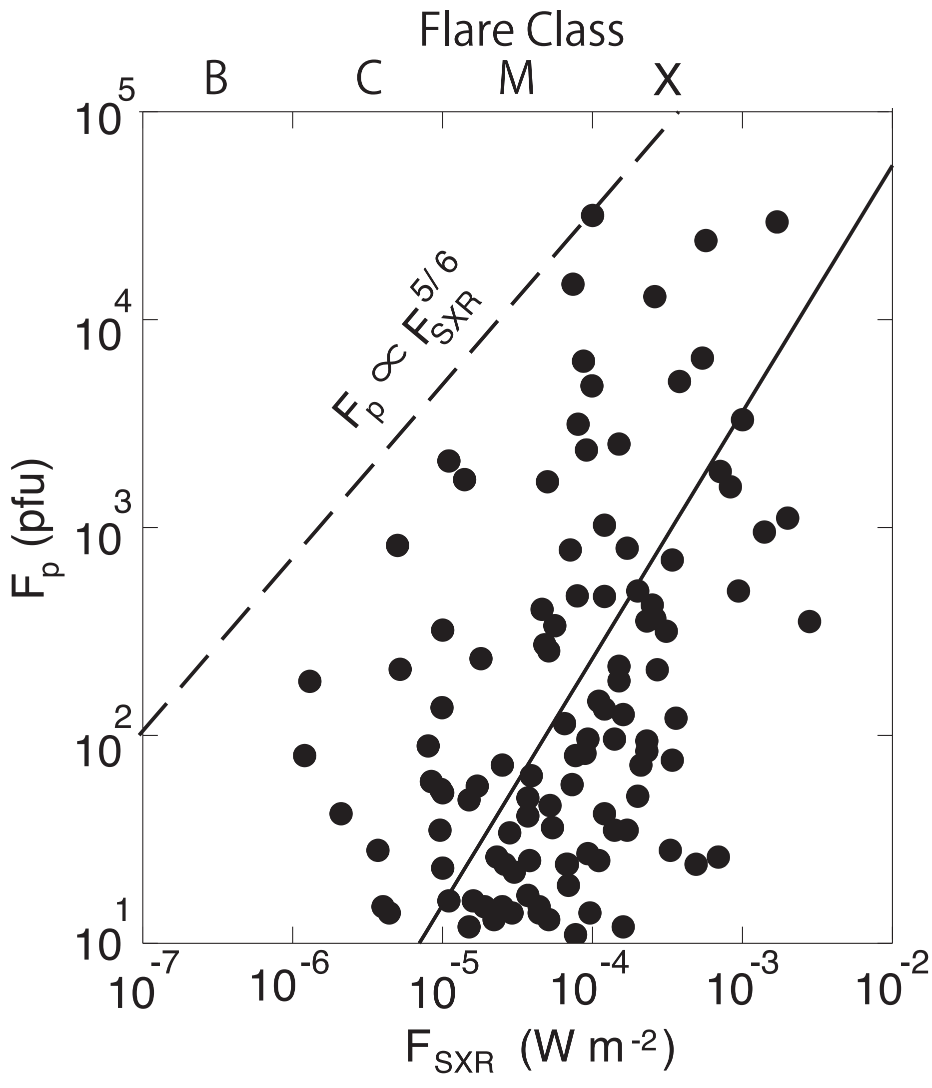

Fig. 1.— F_p-F_{SXR} relation. Solid line is the linear regression fit, of equation $F_p \propto F_{SXR}^{\beta}$ with $\beta = 1.19 \pm 0.08$. The dashed line is the upper limit of F_p in terms of F_{SXR} (equation (10)).

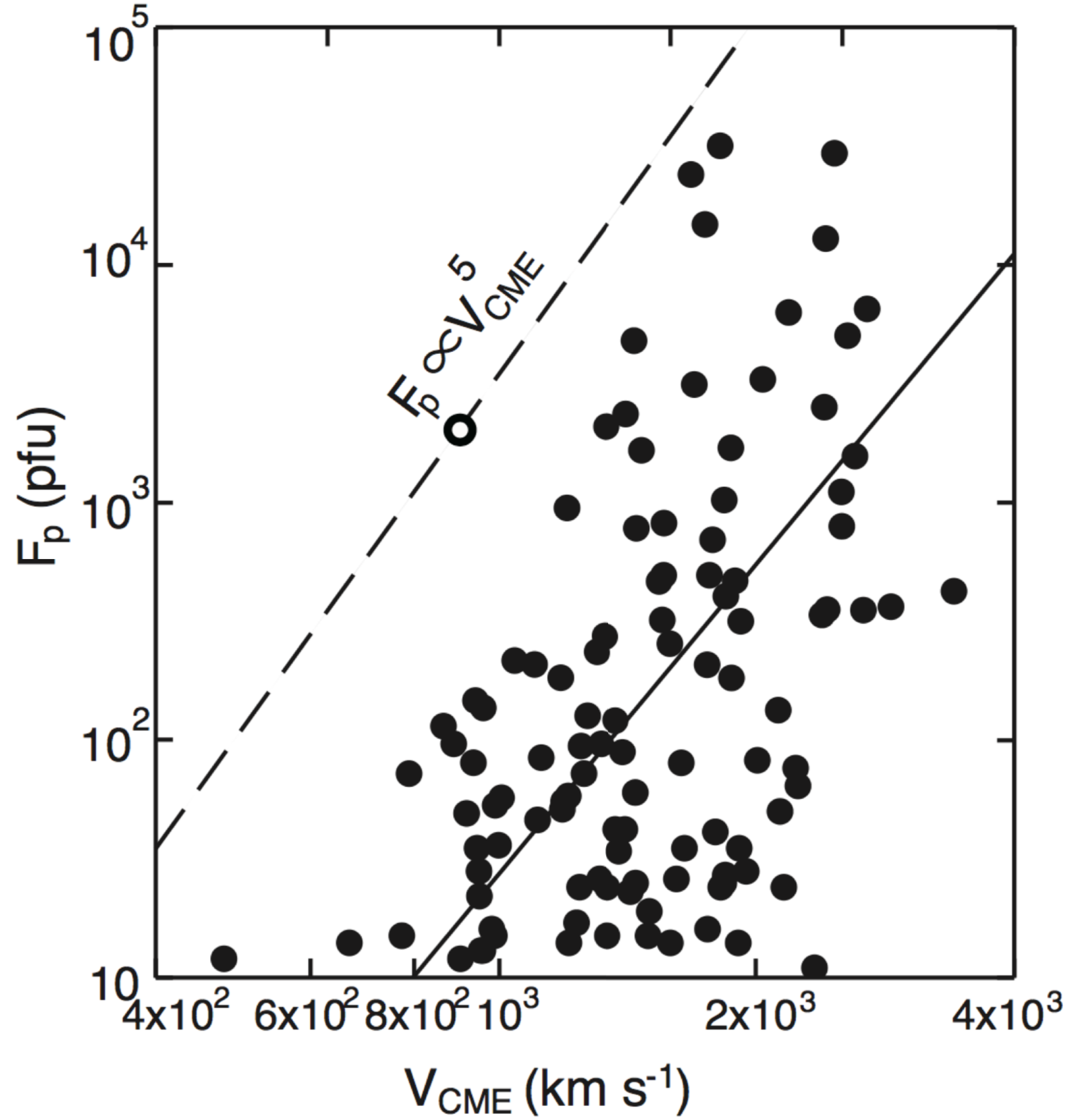

Fig. 2.— F_p-V_{CME} relation. Solid line is the linear regression fit $F_p \propto V_{CME}^{\gamma}$ with $\gamma = 4.35 \pm 0.50$. The dashed line is the upper limit of F_p in terms of V_{CME} whose spectral index is 5. The SPE represented by an unfilled circle in the figure seems to be an outlier, and the linear regression without it made the slope a bit steeper, namely $\gamma = 4.50 \pm 0.48$.

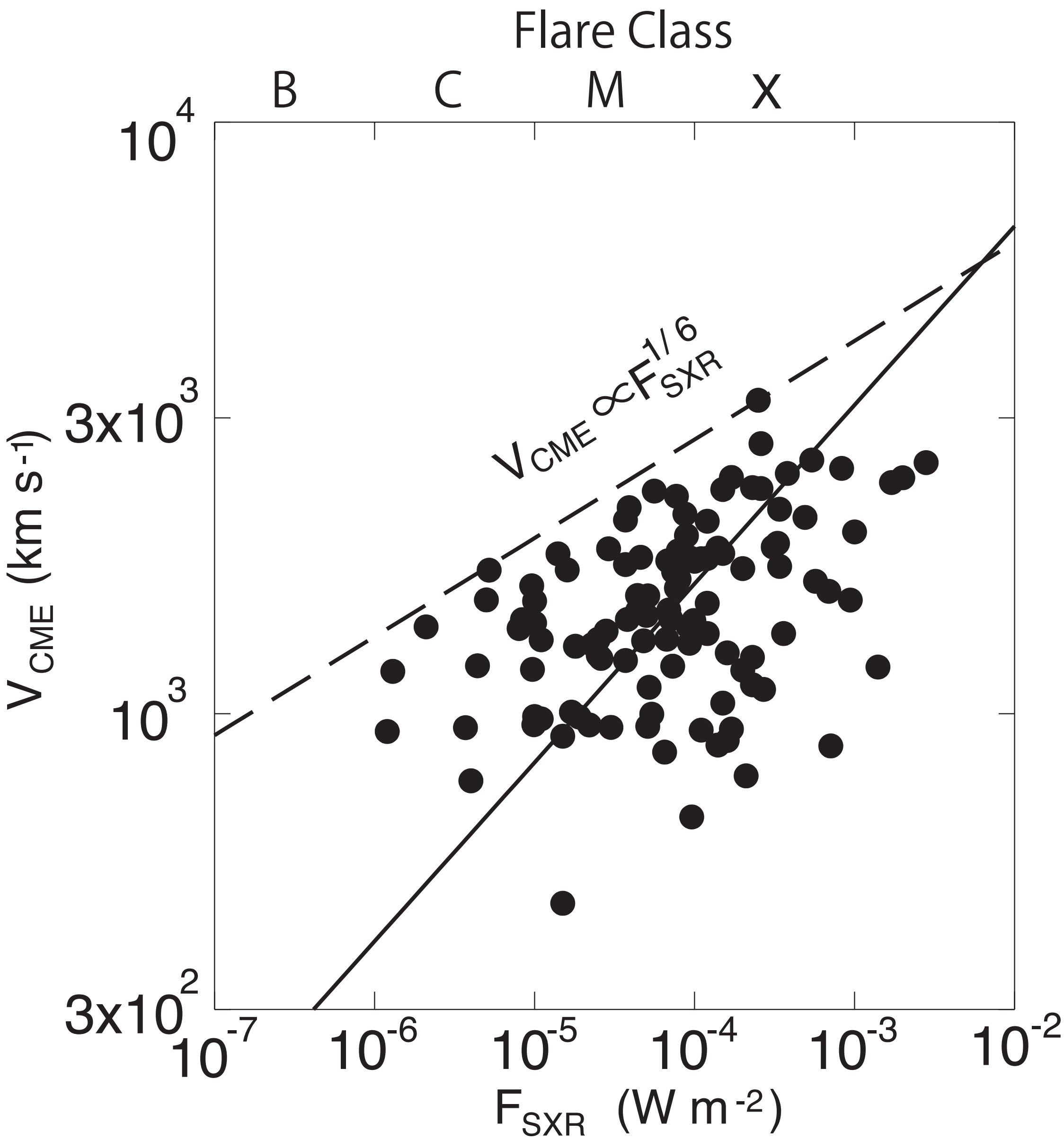

Fig. 3.— V_{CME}-F_{SXR} relation. Solid line is the linear regression fit, of equation $V_{CME} = F_{SXR}^{\alpha}$ with $\alpha = 0.30 \pm 0.04$. The dashed line is the upper limit of V_{CME} in terms of F_{SXR} (equation (7)).

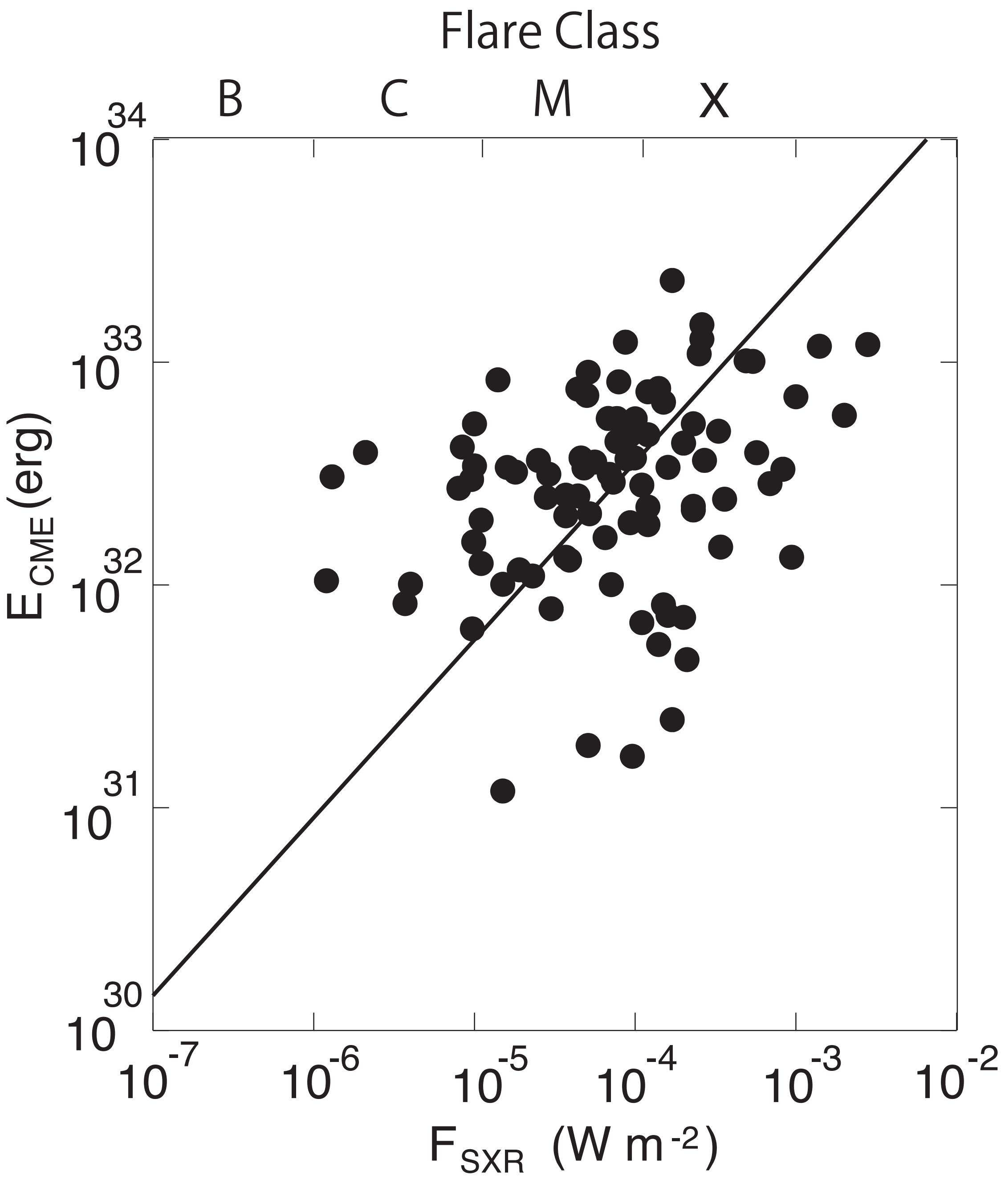

Fig. 4.— E_{CME}-F_{SXR} relation. Solid line is the linear regression fit, of equation $E_{CME} \propto F_{SXR}^{\epsilon}$ with $\epsilon = 0.80 \pm 0.07$.

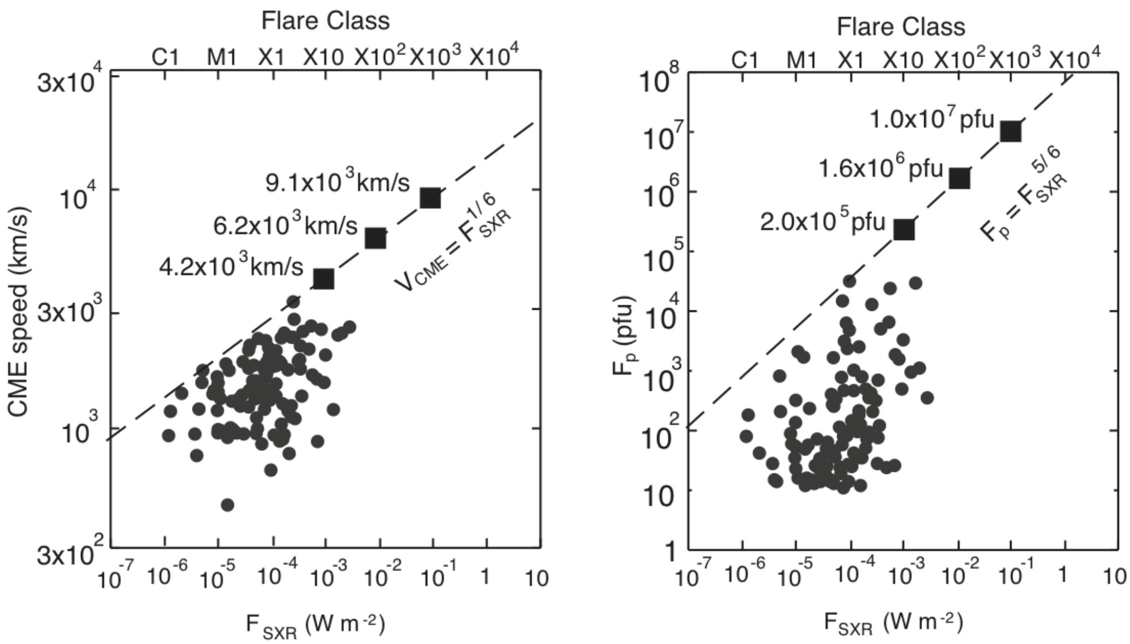

Fig. 5.— (a): V_{CME}-F_{SXR} relation. The estimated upperlimits of CME speed associated with X10, X100 and X1000 class flares are represented as black filled rectangles. (b): F_p-F_{SXR} relation. The estimated upperlimits of energetic proton flux associated with X10, X100 and X1000 class flares are represented as black filled rectangles. The dashed lines in (a) and (b) are the upperlimits of V_{CME} and F_p in terms of F_{SXR} given by equation (4) and (6), respectively.